Case Studies in Thermal Engineering 28 (2021) 101481

Contents lists available at ScienceDirect

Case Studies in Thermal Engineering

journal homepage: www.elsevier.com/locate/csite

Energy, exergy and economics study of a solar/thermal panel cooled by nanofluid

Man-Wen Tian [a], Yacine Khetib [b,c], Shu-Rong Yan [a], Muhyaddin Rawa [c,d], Mohsen Sharifpur [e,f,**], Goshtasp Cheraghian [g,*], Ammar A. Melaibari [b,h]

[a] National Key Project Laboratory, Jiangxi University of Engineering, Xinyu, 338000, China
[b] Mechanical Engineering Department, Faculty of Engineering, King Abdulaziz University, Jeddah, 80204, Saudi Arabia
[c] Center Excellence of Renewable Energy and Power, King Abdulaziz University, Jeddah, 80204, Saudi Arabia
[d] Department of Electrical and Computer Engineering, Faculty of Engineering, King Abdulaziz University, Jeddah, 21589, Saudi Arabia
[e] Department of Mechanical and Aeronautical Engineering, University of Pretoria, Pretoria, 0002, South Africa
[f] Department of Medical Research, China Medical University Hospital, China Medical University, Taichung, Taiwan
[g] Technische Universität Braunschweig, Braunschweig, 38106, Germany
[h] Center of Nanotechnology, King AbdulAziz University, Jeddah, 80204, Saudi Arabia

ARTICLE INFO

Keywords:
Economic analysis
Exergy
Solar panel
Nanofluid
PVT

ABSTRACT

This paper simulates a simple solar panel and the solar panel with a cooling system. The present paper aims to perform an economic and exergy study of PV and PVT 250 W and to compare the return on investment for the operating conditions in China. PVT working fluid is MgO/water nanofluid. PVT cooling system includes a special arrangement of copper tubes placed at its bottom, which cools the panel and produces hot water. COMSOL Multiphysics software and finite element method are employed for numerical analysis and simulation of solar panels. An in-house code is MATLAB code and meteorological data from China are used for economic analysis. The variables include the volume percentage of nanoparticles that is between 0 and 1% and the volume flow rate from 0.5 to 4 lit/min. The results of this study show that enhancing the nanofluid flow in the cooling system makes the panel cooler and reduces the amount of exergy output. The addition of nanoparticles, especially at low nanofluid flow rates, enhances the exergy output. The trend of changes in exergy efficiency with the variations of volume percentage of nanoparticles and volume flow rate is similar to that of the exergy output. The results demonstrate that an increment in the flow rate from 0.5 to 4 lit/min reduces the efficiency by 2.03%. Adding 1% nanoparticles increases the exergy efficiency by 0.45% at a volume flow rate of 0.5 lit/min. The economic analysis of the solar panel shows that the investment recovery is 6 years for PV and 4 years for PVT.

1. Introduction

Energy is one of the serious problems affects the human future. The rising need of energy to provide welfare for human beings has led different countries to explore different energy sources [1,2]. Today, most of the energy needed is provided by fossil fuels.

* Corresponding author.
** Corresponding author. Department of Mechanical and Aeronautical Engineering, University of Pretoria, Pretoria, 0002, South Africa.
E-mail addresses: mohsen.sharifpur@up.ac.za (M. Sharifpur), goshtasbc@gmail.com (G. Cheraghian).

https://doi.org/10.1016/j.csite.2021.101481
Received 29 July 2021; Received in revised form 7 September 2021; Accepted 21 September 2021
Available online 4 October 2021

Consumption of natural fuels has caused widespread pollution on the Earth. Fossil fuels, on the other hand, are a non-renewable resource. Thus, finding a reliable and renewable energy source for the future will be one of the human challenges that will affect many countries [3]. Some countries have replaced their energy sources several years ago. Sources such as wind, sea waves, and the sun are among the renewable resources [4–6]. Meanwhile, solar energy has received more attention than other renewable energy sources [7–11]. Some countries have also made huge investments in this field. Researchers have also investigated this field and have aimed to improve this field of science with their suggestions and studies. Some researchers have done studies on solar collectors, desalination plants, PVs, etc. [12–15]. PVs have attracted the attention of many researchers and many articles have been published [16–19]. The low efficiency of the panels has led researchers to explore different solutions to enhance the efficiency of these devices. One of the effective solutions is to cool the panels using different methods that have been done by different researchers [20]. Meanwhile, using liquids to cool the panel and to heat the house, and convert the panel to a solar water heater is one of the popular methods among researchers. Various investigations have been conducted in this field so far [21]. Khanjari et al. [22] studied a PVT hybrid system

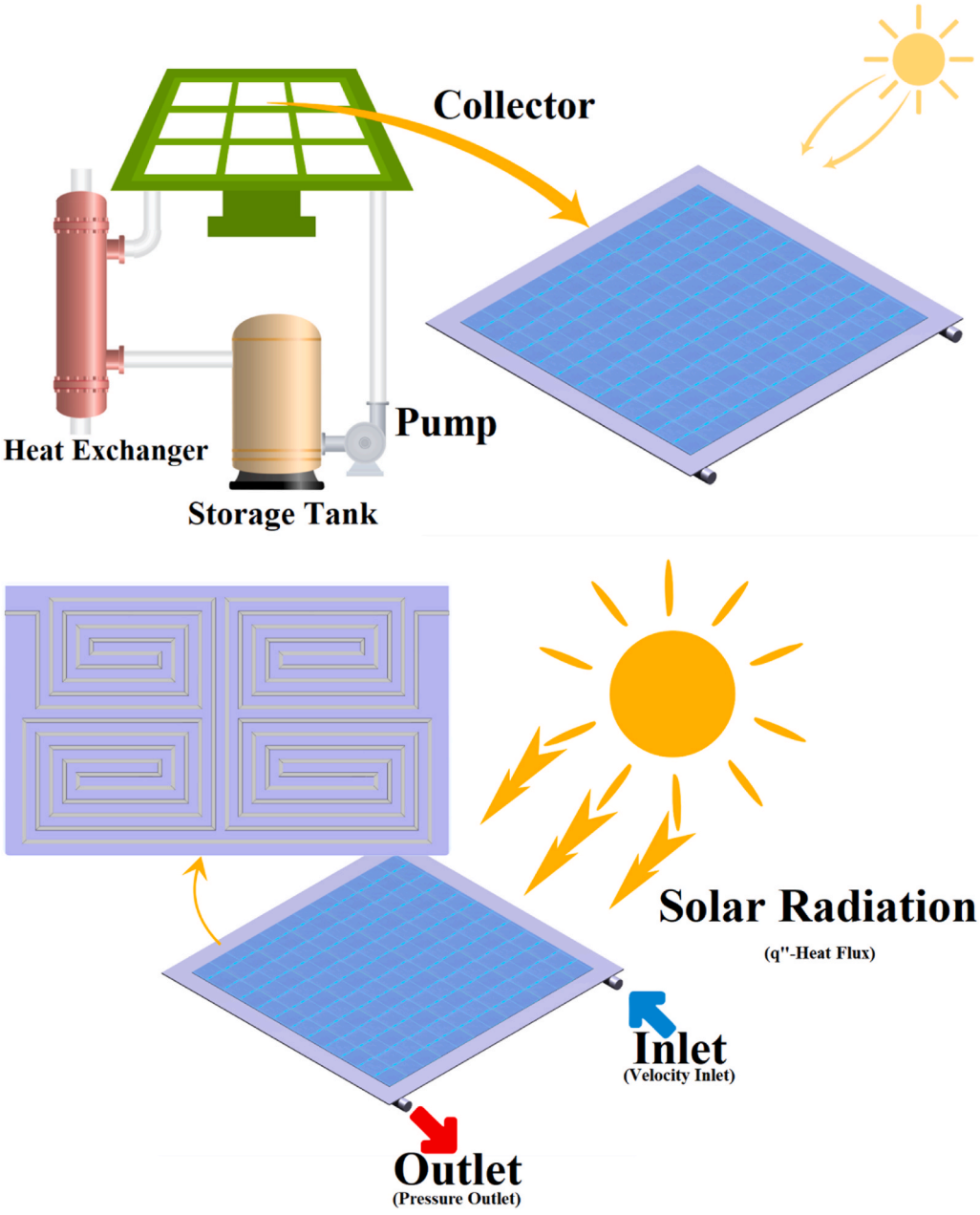

Fig. 1. (a) Schematic of the solar system with PVT.
(b) The arrangement of tubes under the solar panel.

numerically by using liquid as a coolant. The cooling system consisted of a water pipe and an absorber plate. They found that an enhancement in the fluid inlet velocity intensifies the heat transfer efficiency. To study different case studies, the investigators use two experimental and numerical methods in the field of heat transfer. Among them, the numerical method has been considered by many researchers due to its much lower cost than the experimental approach [23–27].

Researchers have employed nano technology in their investigations for more than two decades [28–31]. Nanofluids have been used by researchers in many articles in recent years [32–36]. Many of these studies confirmed that the use of nanofluids can improve heat transfer [37–41]. Nanofluids have been used in enclosures, heat exchangers, air conditioners, heat sinks, etc. [42–46]. Solar devices are one of the equipment in which nanofluids are widely used and many articles have been published in this field [47–51]. Some researchers have also used different nanofluids in PVTs [52–54]. Aberoumand et al. [55] examined a PVT system experimentally. Their system was cooled by a stream of silver/water nanofluid. They found that using nanofluid improves the efficiency of the solar system. They reported that an increment in the percentage of nanoparticles, as well as the nanofluid mass flow rate, improves the efficiency of the system. Due to the importance of studying the exergy of various devices, some researchers also studied the exergy in solar systems, especially PVTs [56,57]. Maadi et al. [29] examined a PVT system in the presence of nanofluids in terms of exergy analysis. They used different nanofluids with different values of φ for cooling and demonstrated that the addition of nanoparticles improves the exergy efficiency.

The importance of solar energy has been well known for researchers since it is permanent, safe, reliable, and available. Among different energy devices, solar panels have become more popular due to their ease of use. However, due to the low cost of electricity in many countries around the world, as well as the inability of these devices to generate electricity for 24 h a day, solar devices are still not widely used in various countries. On the other hand, with the wide range of studies on solar energy, less attention has been paid to the exergy and economic aspects of these devices. Therefore, in this article, the exergy and economic evaluation of a PV and PVT is performed numerically. This study is conducted using meteorological data as well as prices in the Chinese market. The fluid flow in the PVT is MgO/water nanofluid. Finally, the exergy values and the investment recovery time for PV and PVT systems are investigated. For the PVT system, the nanofluid flow rate changes from 0.5 to 4 lit/min, and the percentage of nanoparticles varies up to 1%. The effect of Q on panel temperature is also studied.

2. Problem description

The solar panel (Fig. 1) is a 250-W panel with dimensions of 163.8 cm × 99.2 cm. The present study evaluates a simple panel and the one with a cooling system (PVT). The PVT (Fig. 1) system operates in a cycle that provides hot water. A schematic of this cycle is given in Fig. 1a. To fabricate the PVT system, a heat exchanger is placed under the panel. The heat exchanger consists of a copper plate with a diameter of 12.88 mm and a length of 13.5 m, which is located with a special arrangement at the rear of the panel. MgO/water nanofluid flows in the tubes. The variables include the volume percentage of nanoparticles ranging from 0.1 to 1% and the volume flow rates of 0.5–4 lit/min.

2.1. Governing equations

The governing equations for.
Newtonian, incompressible, and homogeneous fluid.
Laminar and steady flow.
Gravity and viscosity loss are neglected.
The interaction forces between nanoparticles and fluid are ignored.
can be expressed as follows [58,59]:

$$\nabla.\left(\rho_{\mathrm{nf}} v\right) = 0 \tag{1}$$

$$\nabla.\left(\rho_{\mathrm{nf}} vv\right) = -\nabla P + \nabla.\left(\mu_{\mathrm{nf}} \nabla v\right) \tag{2}$$

$$\nabla.\left(\rho_{\mathrm{nf}} v \mathrm{c}_{\mathrm{p,nf}} T\right) = \nabla.\left(k_{\mathrm{nf}} \nabla \mathrm{T}\right) \tag{3}$$

$$\nabla.\left(k^{*} \nabla \mathrm{T}\right) = 0 \tag{4}$$

The values of v, P, and T represent velocity, pressure, and temperature, respectively. Besides, ρ is the density, k thermal conductivity, $c_p$specific heat capacity and μ is dynamic viscosity. The nf index refers to the nanofluid and $k^*$is the thermal conductivity of the solid.

2.2. Nanofluid equations

In this paper, MgO/water nanofluid is used as a working fluid in the solar cycle. The thermal conductivity nanofluid is calculated using the correlation presented by Esfe et al. [60] based on experimental data:

$$\frac{k_{nf}}{k_{bf}} = 1.1507 + 0.05\varphi - 0.013d_p + 0.0038T - 0.0049\varphi d_p + 0.0006\varphi T - 0.0019d_pT - 0.0057\varphi^2 - 0.0012T^2 - 0.0013\varphi d_pT + 0.0013\varphi^2 d_p \quad (5)$$

where bf represents the base fluid (water), d_p is nanoparticle diameter which is equal to 40 nm and φ is the volume percentage of nanoparticles. Also, to estimate the viscosity, another experimental model is used, which has been presented by Khodadadi et al. [61]:

$$\frac{\mu_{nf}}{\mu_{bf}} = 11.938 + 0.258e^{\varphi^{1.077}} - 2.286e^{T^{0.266}} + 0.679T \quad (6)$$

Other required properties of nanofluids and their relationships are as follows:

$$\rho_{nf} = (1-\varphi)\rho_f + \varphi\rho_p \quad (7)$$

$$(\rho c_p)_{nf} = (1-\varphi)(\rho c_p)_f + \varphi(\rho c_p)_p \quad (8)$$

The values of properties are given in Table 1 for water and MgO.

2.3. Exergy analysis

The following equation represents the relation between output, input, and exergy loss [64–66]:

$$E_{x\ in} - E_{x\ out} = E_{x\ loss} \quad (9)$$

The exergy efficiency can be expressed using the following equation, i.e. the ratio of the total output exergy to the total input one [64–66]:

$$\eta_{ex} = \frac{E_{x_{output}}}{E_{x_{input}}} \quad (10)$$

For the solar panel, input exergy is [64–66]:

$$E_{x_{in}} = A \times G \times \left[1 - \frac{4}{3}\left(\frac{T_a}{T_s}\right) + \frac{1}{3}\left(\frac{T_a}{T_s}\right)^4\right] \quad (11)$$

Index *a* represents the environment and index *s* represents the panel surface.
Output exergy is also defined as follows, i.e. the sum of thermal exergy and electrical one [67]:

$$E_{x_{out}} = E_{x_{thermal}} + E_{x_{electrical}} \quad (12)$$

Since the amount of electricity received from the panel is the output exergy, it is necessary to calculate the thermal exergy, which can be calculated from the following relation [67]:

$$E_{x_{thermal}} = \mathscr{Q}\left[1 - \frac{T_a}{T_c}\right] \quad (13)$$

The value of Q can be obtained as follows [67]:

$$\mathscr{Q} = UA(T_c - T_a) \quad (14)$$

where *U* is the overall heat transfer coefficient, which for the panel includes radiation heat transfer coefficient and convective heat transfer coefficient, and is obtained using the following equation [67]:

$$U = h_{conv} + h_{rad} \quad (15)$$

The convective heat transfer coefficient is [67]:

$$h_{conv} = 2.8 + 3v \quad (16)$$

Where *v* is the wind speed. The radiation heat transfer coefficient between the solar panel and the surrounding can be obtained using the following equations [65]:

Table 1
Properties of water and MgO nanoparticles [62,63].

	C_P(J/kg.k)	k(w/m.k)	ρ(kg/m^3)	μ(kg/m.s)
Water	4179	0.613	997.1	0.001
MgO	937	54.9	3580	–

$$h_{rad-1} = \varepsilon\sigma\left(T_{sky} + T_c\right)\left(T_{sky}^2 + T_c^2\right) \tag{17}$$

$$h_{rad-2} = 1.78(T_m - T_a) \tag{18}$$

To obtain the values of radiative heat transfer coefficient, it is necessary to determine the sky temperature, which can be calculated as follows [65]:

$$T_{sky} = T_a - 6 \tag{19}$$

Finally, the relation between the surface temperature of the solar collector can be written as follows [68,69]:

$$T_c = \frac{P_{sg}G\left(\tau_g\alpha - \eta_{el}\right) + \left(h_{conv}T_a + h_{rad-2}T_b\right)}{h_{conv} + h_{rad-2}} \tag{20}$$

where $P_{sg}$is the value of the packing factor for the solar module and index b represents the back of the panel.

The inflow exergy for the collector surface is [65,70]:

$$\sum E_{in} - \sum\left(E_{x_{th}} + E_{x_{pv}}\right) = \sum E_{x_d} \tag{21}$$

$$E_{x_{th}} = \mathscr{C}_u\left(1 - \frac{T_a + 273}{T_o + 273}\right) \tag{22}$$

$$E_{x_{pv}} = \eta_{pv} \times A \times N_c \times G \times \left[1 - \frac{4}{3}\left(\frac{T_a}{T_s}\right) + \frac{1}{3}\left(\frac{T_a}{T_s}\right)^4\right] \tag{23}$$

$$E_{x_{PVT}} = E_{x_{th}} + E_{x_{pv}} \tag{24}$$

where E_{in} is input exergy, $E_{x_{pv}}$ is panel exergy, $E_{x_{th}}$ is thermal exergy, $E_{x_{PVT}}v$ is PVT exergy, N_c is the number of collectors, T_s is solar temperature and E_{x_d} is exergy destruction.

Finally, the exergy efficiency can be expressed as follows [65,70]:

$$\eta_{ex} = 1 - \frac{E_{x_d}}{E_{x_{in}}} \tag{25}$$

All the constant values required in the above relations can be seen in Table 2.

2.4. Economic analysis

Annual worth (AW) is the difference between profit (income) and annual expenses [71,72]:

$$A.W = B_A - C_A \tag{26}$$

where B_A is annual income and C_A is an annual cost.

The annual value relation for the solar system can be defined as follows [64]:

$$(A.W)_{PV_{Solar}} = -\left(I_C + I_{IC}\right)(A/P, i, N) - A_{rc} - \left(C_{afic}\right)(A/F, i, N) \tag{27}$$

where I_C is the initial cost, I_{IC} is the installation cost, A/P is the recovery factor, i is the interest rate, N is the lifetime, A_{rc} is the annual

Table 2
Constant values for exergy relations [65,70].

Symbol	Value
A, A_c	1.64
N_1, N_c	1
ε_g	0.88
ε_p	0.95
β	15
C_P	4185.5
T_s	5777
v	1.1
τ	0.96
α	0.90
P_{sg}	0.8

cost, A/F is the change of aluminum coating.

To solve the above equations, any one-time payment or income must be converted into an equivalent period using the recovery factors $A/P, i, N$ and A/F. Hence [71,72]:

$$A \Big/ P = \frac{i(1+i)^N}{(1+i)^N - 1} \tag{28}$$

$$A \Big/ F = \frac{i}{(1+i)^N - 1} \tag{29}$$

3. Numerical solution method and boundary conditions

COMSOL Multiphysics 5.4 software and finite element method are employed for simulating nanofluid flow and thermal solution. First, the PVT geometry is sketched and meshed using COMSOL Multiphysics software. The grid generation is done using hexagonal elements. An example of a grid on a PVT heat exchanger is shown in Fig. 2. Then, the equations are solved by using the radiation and heat transfer modules. For economic studies, an in-house code is employed using MATLAB software. The economic analysis is performed using COMSOL Multiphysics software outputs and China weather data. The amount of heat flux applied to the panel is assumed to be 500 W/m^2. The fluid enters the tube at a constant velocity and temperature of 293 K and exits at a constant pressure.

4. Grid independence test and validation

To solve the governing equations, it is necessary to perform a grid study. Hence, the maximum panel temperature is calculated for Q = 4 lit/min and different grid resolutions. The results are given in Table 3. According to the table, it can be seen that there are no changes in the results when the number of elements is larger than 3.8 million; thus, this grid is selected for further simulations.

To verify the present simulations, the Nusselt number is calculated and compared with the results of Saffarian et al. [73] who studied a solar collector at different Reynolds numbers (Fig. 3), indicating that the present simulations result in reasonable results. In the above article, the impact of different tube arrangements on the efficiency of a solar collector was investigated. They used alumina/water and copper oxide/water nanofluids for their research. In the figure, the values of the Nusselt number are calculated for different Reynolds numbers and compared with the results reported by this paper. The comparison is performed for the collector with a U-shaped tube arrangement.

5. Results and discussion

The results are discussed in three sections: thermal, exergy, and economic analysis.

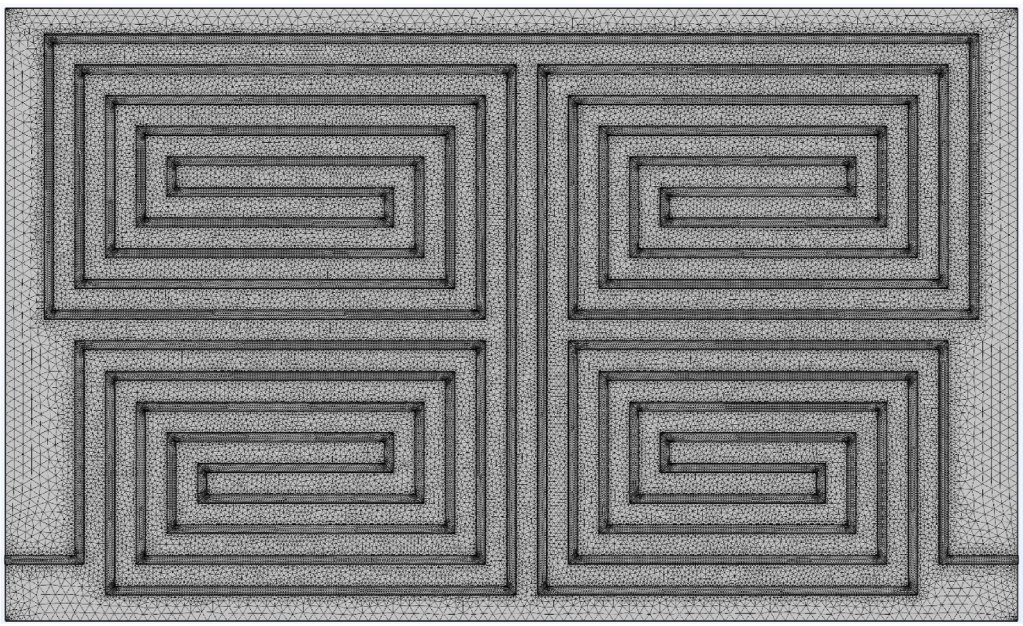

Fig. 2. An example of a grid stacked for PVT geometry.

Table 3
Maximum panel temperature for Q = 4 lit/min and different grid resolutions.

Number of elements (million)	2.1	2.6	3.0	3.4	3.8	4.3
Maximum panel temperature	315.17	309.87	307.54	305.64	305.12	305.09

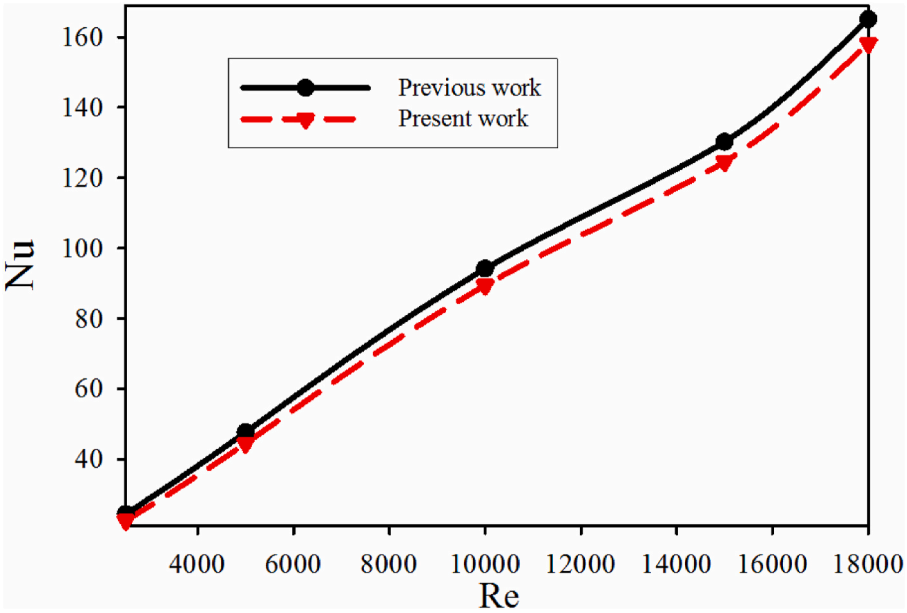

Fig. 3. Nusselt number as a function of Reynolds number.

5.1. PVT thermal analysis

Fig. 4 demonstrates the temperature contours for the solar panel when the flow rate is 0.5 and 4 lit/min. It can be seen that the panel has a lower temperature at the inlet and a higher temperature at the outlet. Due to the special arrangement of the tubes, the panel becomes warmer when water flows in the tubes and its temperature is increased. An increment in the temperature leads to that the fluid does not receive considerable heat from the panel, so the panel gets warmer. At a higher flow rate, the panel is significantly colder than the panel with a lower water flow rate so that the maximum temperature of the panel is dropped sharply. Enhancing the water flow causes the fluid to circulate faster in the tubes and collides with the tubes at a lower temperature compared to lower flow rates. Hence, water can cool the panel properly. Also, higher flow rates of water lead to that it exits the solar panel at a lower temperature.

5.2. Exergy analysis

Fig. 5 shows the output exergy for water and nanofluid with $\varphi = 3\%$ and different values of Q. It can be seen that the addition of nanoparticles to water intensifies the amount of output exergy. The increment in the temperature at the outlet is the most important reason for this enhancement in fluid temperature at the outlet. The difference between the fluid temperature at the outlet and the ambient temperature enhances the workability of the fluid and as a result the amount of exergy. As the output temperature of the fluid reaches the ambient temperature, it reaches the dead state and the amount of fluid exergy becomes zero. Initially, a sudden increase is observed in exergy output by adding 0.1% nanoparticles. The addition of more nanoparticles leads to that the increase in exergy output has a smaller trend. At lower volume flow rates, the increase in exergy output is higher. The addition of nanoparticles reduces the heat capacity of the fluid, which causes the addition of nanoparticles to enhance the exergy output by up to 1%. At a flow rate of 4 lit/min, adding 1% nanoparticles reduces the amount of exergy compared to 0.1% nanoparticles. An increment in the flow rate leads to a permanent decreasing trend in the exergy. Enhancing the fluid velocity causes the fluid to have less time to exchange heat with the panel and as a result, its temperature enhancement is reduced. Thus, the exergy output decreases at higher flow rates. However, at higher flow rates, the decreasing trend of exergy is reduced with the flow rate.

Fig. 6 demonstrates the exergy efficiency for water and nanofluid with $\varphi = 3\%$ and different amounts of Q. It can be seen that the amount of exergy efficiency for the solar panel is low. For the best case, i.e. $\varphi = 1\%$ and Q = 0.5 lit/min, the exergy efficiency is less than 13%. An increment in the Q from 0.5 to 4 lit/min reduces this amount so that the amount of exergy efficiency changes from 11.9% to 9.87%. The addition of nanoparticles is generally enhanced the amount of exergy efficiency. The highest increase in exergy efficiency corresponds to low values of Q. The addition of 1% nanoparticles intensifies the amount of exergy is improved by 0.45% at Q =

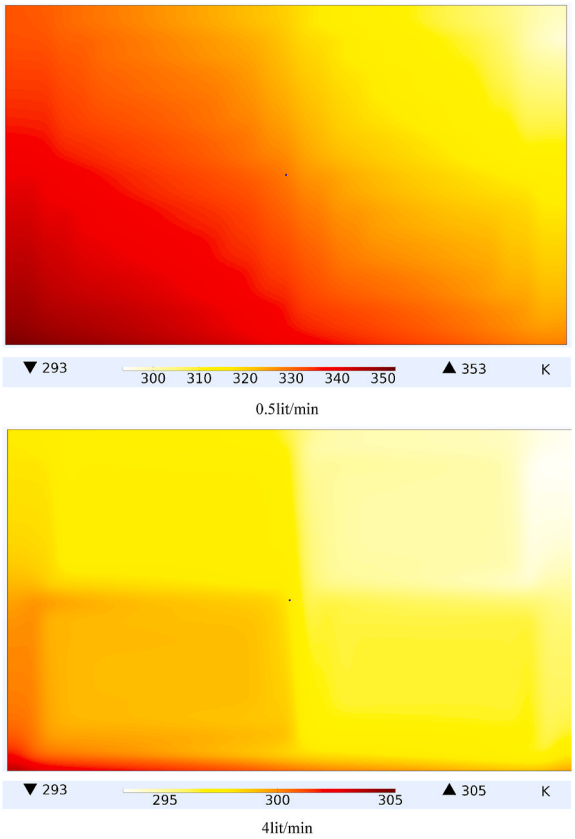

Fig. 4. Temperature contours on the solar panel at Q = 0.5 and 4 lit/min.

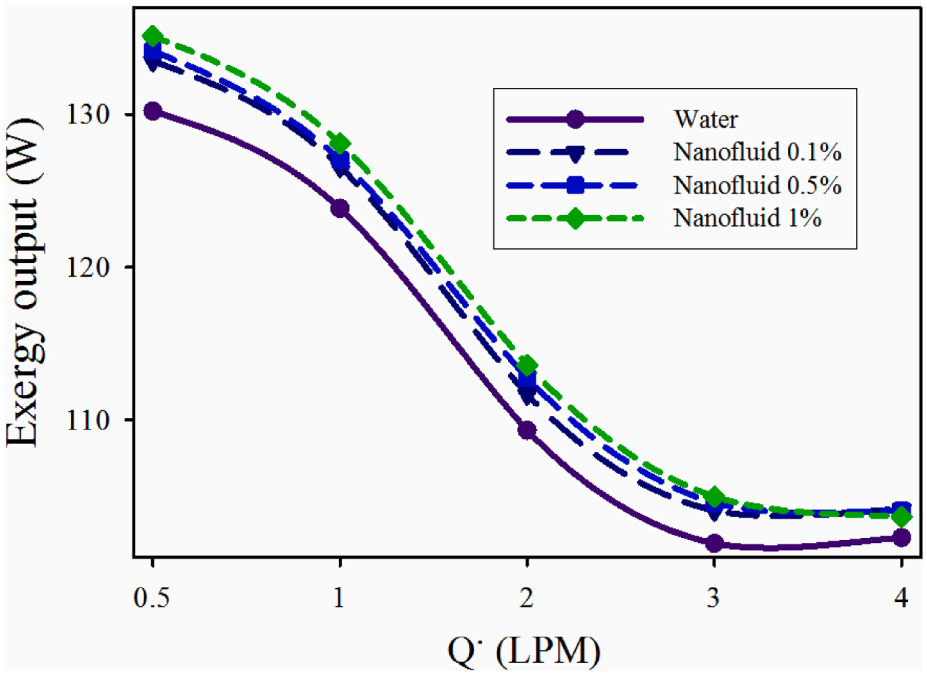

Fig. 5. Output exergy for water and nanofluid with φ = 3% and different values of Q.

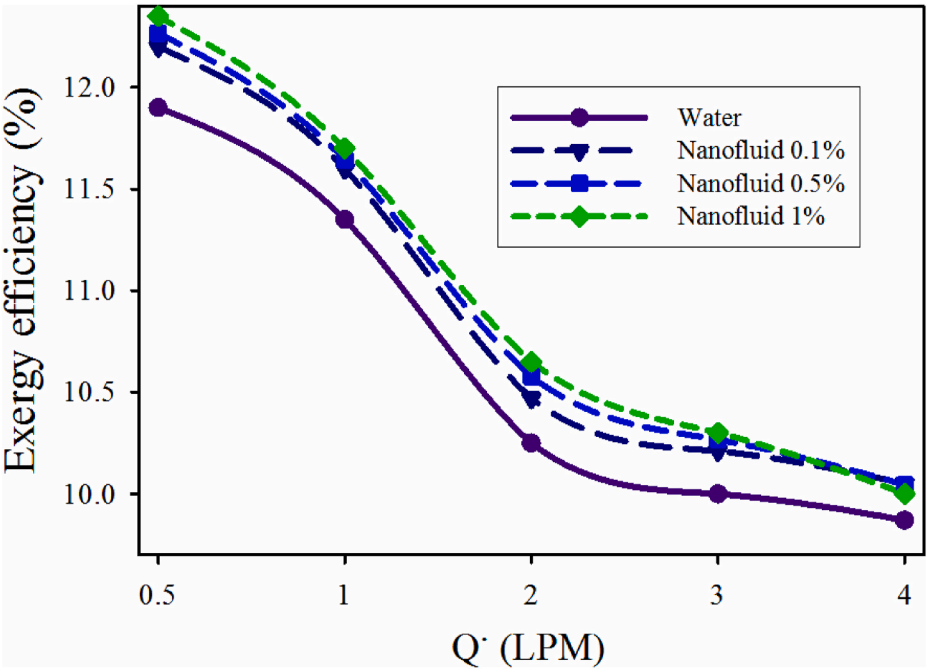

Fig. 6. Exergy efficiency for water and nanofluid with φ = 3% and different values of Q.

0.5 lit/min. As the distance between the outlet temperature and the ambient temperature increases, the exergy is enhanced, leading to reach a higher temperature than the dead state and a greater amount of fluid workability. Hence, the fluid temperature can be used for different applications. The addition of nanoparticles causes to reach a state far from the dead state and as a result, more workability can be obtained for the nanofluid.

5.3. Economic analysis

Solar energy systems are generally classified in the group of high initial cost and low operating costs in comparison with water heaters and electric systems which have a relatively low initial cost and high operating costs. Solar water heating is highly efficient over a long period. One of the main reasons is the lack of fuel requirement and its cost preparations. Besides, a side effect of using solar systems is environmental protection. The cost-benefit analysis is based on the annual worth method, which consists of two parts, in which case the cost of a solar system is compared to the cost of an electric water heater. The electricity produced in the cell is also analyzed separately. Current costs in China are used to purchase equipment, as well as installation and maintenance costs. These costs

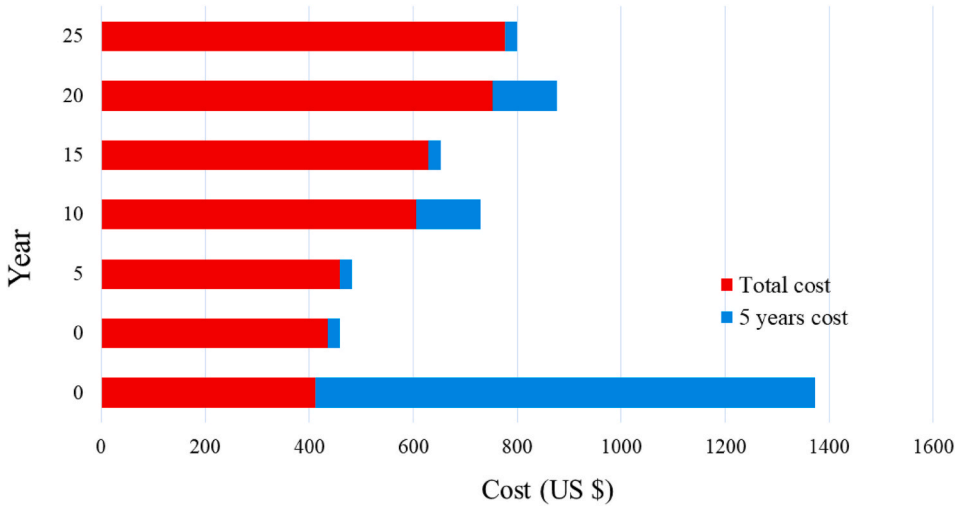

Fig. 7. Cash flow diagram for PV system from the installation time until 25 years later.

are expressed in US dollars.

5.3.1. Economic analysis of a PV system

An economic analysis typically discusses the system repayment period or the time of investment recovery of the system. In this work, two modes are analyzed: the solar PV panel and the PVT system with the nanofluid flow. This analysis gives a clear understanding of the period of investment recovery for the two systems. For this purpose, equations (26)–(29) are employed and the system is analyzed by drawing a flow diagram. A cash flow diagram is drawn in Fig. 7 for the solar panel system. Using the results of meteorological data [74]for China, it can be predicted that the investment cost will return in a 6-year period. Calculations are done by considering the 10% interest. Finally, these results are obtained using some assumptions.

Fig. 7 reveals the cash flow diagram of a PV module from the installation time until 25 years later. In this figure, the 5-year cost is considered and also the total cost in each 5-year period is given. Maintenance cost is considered as much as 23.46$ for each 5-year period. The cost is zero in the first year and is 23.45$ for the installation cost. Also, the cost of fuel is considered zero. The cost of the panel and its equipment is estimated 411.25$. Also, the amount of 100$ is considered for the general maintaining of the solar panel system for 10-year periods. To calculate the annual interest, the average PV output for 6 h is calculated using the annual Chinese weather data [74]. This interest for a 6-year period of the panel is 123.06 $. Also, considering the cost of 1 kWh of electricity in China, which is 0.084 $/kWh for home use [75], the calculations are performed for the 6-year initial costs.

5.3.2. Economic analysis of PVT system with nanofluid flow cooling

The cost of purchase and insulation of the solar panel and the cost of nanofluid for a PVT system is estimated as 422.22 $ and 540 $, respectively [76]. This amount of nanofluid is required for the system to work so that the minimum value of nanofluid required is 4 L. Fig. 8 demonstrates a PVT cash flow diagram cooled with a nanofluid from start-up until 25 years later. The costs are given at different years. Costs include purchasing and installing the initial system as well as the cost of purchasing nanofluids. Also, during the 5-year period, considering the sedimentation of nanoparticles, an additional cost plus 5-year maintenance cost are added, which is 445 $. The initial installation cost is the same as the previous system, i.e. 23.64 $. Also, the current cost of the system is zero per year.

To calculate the annual interest, the simulation results, as well as meteorological data, are considered for 6 h in a day. Due to the higher efficiency of the PVT system, the investment recovery time is reduced to 4 years. This is acceptable due to the higher cost of this system compared to a simple panel. Finally, by performing economic analysis and also an enhancement in the life of the panel due to its cooling, it is concluded that the PVT system can be used for more years than PV due to its higher advantages.

6. Conclusions

In the present paper, PV and PVT systems are simulated and their exergy and economic analysis is performed. The working fluid of the PVT system is MgO/water nanofluid flowing in a specific arrangement of copper tubes. By changing the Q and φ, the amount of exergy output, exergy efficiency, and investment recovery time are analyzed and the following results are obtained.

1 An increment in the working flow rate in the heat exchanger system in PVT, cools more the panel.
2 Enhancing the fluid flow rate in the heat exchanger system in PVT reduces exergy output. Increasing the volume percentage of nanoparticles enhances the exergy output. The maximum exergy output is obtained for 1% nanofluid at a flow rate of 0.5 lit/min.
3 An enhancement in the fluid flow rate of the heat exchanger system in PVT reduces the exergy efficiency so that increasing the water flow rate from 0.5 to 4 lit/min reduces the exergy efficiency by 2.03%.
4 The addition of nanoparticles enhances the exergy efficiency so that adding 1% MgO to water at a flow rate of 0.5 lit/min enhances the exergy efficiency by 0.45%.
5 Maintenance cost and the initial cost of PVT system is more than PV, while investment recovery is 6 years for PV and 4 years for PVT.

According to the case study, i.e. China, this study can be done for different countries to obtain estimation for the efficiency of solar systems economically. Besides, other cooling systems can be evaluated for the solar panel to investigate its effect on PVT exergy output.

Authors' contributions

Man-Wen Tian: Funding acquisition; Writing - original draft.
Yacine Khetib: Formal analysis; Writing - review & editing.
Shu-Rong Yan: Writing - review & editing.
Muhyaddin Rawa: Writing - review & editing.
Mohsen Sharifpur: Conceptualization.
Goshtasp Cheraghian: Conceptualization; Review & editing.
Ammar A. Melaibari: Formal analysis.

Declaration of competing interest

We wish to confirm that there are no known conflicts of interest associated with this publication and there has been no significant

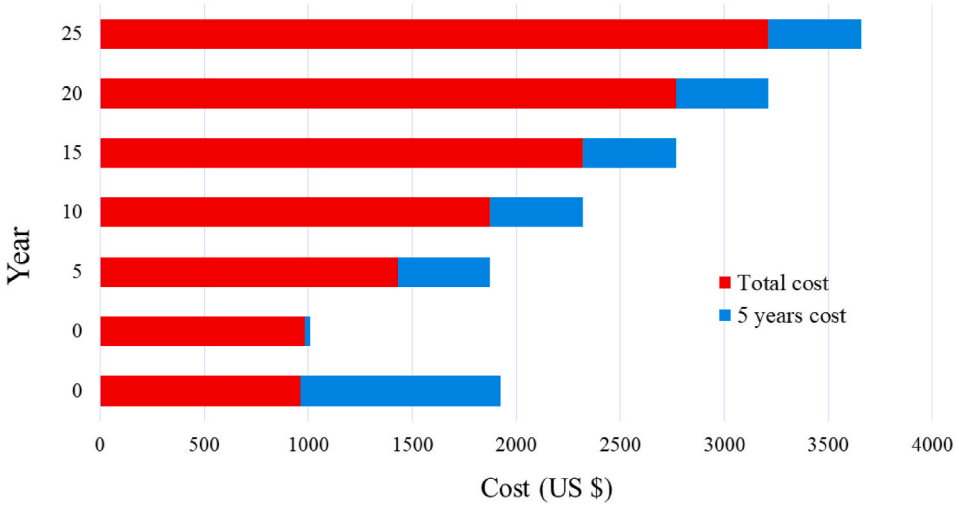

Fig. 8. Cash flow diagram for PVT system from the installation time until 25 years later.

financial support for this work that could have influenced its outcome.

Acknowledgment

"This project was funded by the Deanship of Scientific Research (DSR) at King Abdulaziz University, Jeddah, under grant no. (RG-11-135-40). The authors, therefore, acknowledge with thanks DSR technical and financial support".

References

[1] C. Lamnatou, D. Chemisana, Photovoltaic/thermal (PVT) systems: A review with emphasis on environmental issues, Renew. Energy 105 (2017) 270–287.
[2] A.H. Pordanjani, S. Aghakhani, M. Afrand, M. Sharifpur, J.P. Meyer, H. Xu, et al., Nanofluids: physical phenomena, applications in thermal systems and the environment effects- a critical review, J. Clean. Prod. (2021), 128573.
[3] H. Caliskan, Energy, exergy, environmental, enviroeconomic, exergoenvironmental (EXEN) and exergoenviroeconomic (EXENEC) analyses of solar collectors, Renew. Sustain. Energy Rev. 69 (2017) 488–492.
[4] H. Panchal, K.K. Sadasivuni, Experimental investigation on solar still with nanomaterial and dripping arrangement, Energy Sources, Part A Recovery, Util. Environ. Eff. (2020) 1–11.
[5] H. Panchal, R. Sathyamurthy, A.E. Kabeel, S.A. El-Agouz, D. Rufus, T. Arunkumar, et al., Annual performance analysis of adding different nanofluids in stepped solar still, J. Therm. Anal. Calorim. 138 (2019) 3175–3182.
[6] R. Sathyamurthy, A.E. Kabeel, E.-S. El-Agouz, D. Rufus, H. Panchal, T. Arunkumar, et al., Experimental Investigation on the Effect of MgO and TiO2 Nanoparticles in Stepped Solar Still, vol. 43, 2019, pp. 3295–3305.
[7] C. Jiang, Y. Fang, W. Zhang, X. Song, J. Lang, L. Shi, Y. Tang, A multi-ion strategy towards rechargeable sodium-ion full batteries with high working voltage and rate capability, Angew. Chem. 57 (50) (2018) 16370.
[8] A. Yu, Q. Pan, M. Zhang, D. Xie, Y. Tang, Fast rate and long life potassium-ion based dual-ion battery through 3D porous organic negative electrode, Adv. Funct. Mater. 30 (24) (2020), 2001440, https://doi.org/10.1002/adfm.202001440.
[9] G. Chen, F. Zhang, Z. Zhou, J. Li, Y. Tang, A flexible dual-ion battery based on PVDF-HFP-modified gel polymer electrolyte with excellent cycling performance and superior rate capability, Advanced energy materials 8 (25) (2018), 180121.
[10] H.A. Zondag, Flat-plate PV-Thermal collectors and systems: A review, Renew. Sustain. Energy Rev. 12 (2008) 891–959.
[11] G. Palanikumar, S. Shanmugan, V. Chithambaram, S. Gorjian, C.I. Pruncu, F.A. Essa, et al., Thermal investigation of a solar box-type cooker with nanocomposite phase change materials using flexible thermography, Renew. Energy 178 (2021) 260–282.
[12] D. Zhu, B. Wang, H. Ma, H. Wang, Evaluating the vulnerability of integrated electricity-heat-gas systems based on the high-dimensional random matrix theory, CSEE Journal of Power and Energy Systems 6 (4) (2020) 878–889, https://doi.org/10.17775/CSEEJPES.2019.00440.
[13] M. Vaka, R. Walvekar, A.K. Rasheed, M. Khalid, H. Panchal, A review: emphasizing the nanofluids use in PV/T systems, IEEE Access 8 (2020) 58227–58249.
[14] H. Panchal, H. Nurdiyanto, K.K. Sadasivuni, S.S. Hishan, F.A. Essa, M. Khalid, et al., Experimental investigation on the yield of solar still using manganese oxide nanoparticles coated absorber, Case Studies in Thermal Engineering 25 (2021), 100905.
[15] P. Thamizharasu, S. Shanmugan, S. Gorjian, C.I. Pruncu, F.A. Essa, H. Panchal, et al., Improvement of Thermal Performance of a Solar Box Type Cooker Using SiO_2/TiO_2 Nanolayer. Silicon, 2020.
[16] A. Kasaeian, G. Nouri, P. Ranjbaran, D. Wen, Solar collectors and photovoltaics as combined heat and power systems: A critical review, Energy Convers. Manag. 156 (2018) 688–705.
[17] R. Nadda, A. Kumar, R. Maithani, Efficiency improvement of solar photovoltaic/solar air collectors by using impingement jets: A review, Renew. Sustain. Energy Rev. 93 (2018) 331–353.
[18] A.J. Chamkha, F. Selimefendigil, M.A. Ismael, Mixed convection in a partially layered porous cavity with an inner rotating cylinder, Numer. Heat Tran., Part A: Applications 69 (2016) 659–675.
[19] K. Pansal, B. Ramani, K.k. Sadasivuni, H. Panchal, M. Manokar, R. Sathyamurthy, et al., Use of solar photovoltaic with active solar still to improve distillate output: A review, Groundwater for Sustainable Development 10 (2020), 100341.
[20] S. Shittu, G. Li, Y.G. Akhlaghi, X. Ma, X. Zhao, E. Ayodele, Advancements in thermoelectric generators for enhanced hybrid photovoltaic system performance, Renew. Sustain. Energy Rev. 109 (2019) 24–54.
[21] A. Kumar, P. Baredar, U. Qureshi, Historical and recent development of photovoltaic thermal (PVT) technologies, Renew. Sustain. Energy Rev. 42 (2015) 1428–1436.

[22] Y. Khanjari, F. Pourfayaz, A.B. Kasaeian, Numerical investigation on using of nanofluid in a water-cooled photovoltaic thermal system, Energy Convers. Manag. 122 (2016) 263–278.
[23] T.M.O. Diallo, M. Yu, J. Zhou, X. Zhao, S. Shittu, G. Li, et al., Energy performance analysis of a novel solar PVT loop heat pipe employing a microchannel heat pipe evaporator and a PCM triple heat exchanger, Energy 167 (2019) 866–888.
[24] A. Faddouli, H. Labrim, S. Fadili, A. Habchi, B. Hartiti, M. Benaissa, et al., Numerical analysis and performance investigation of new hybrid system integrating concentrated solar flat plate collector with a thermoelectric generator system, Renew. Energy 147 (2020) 2077–2090.
[25] R. Ye, P. Liu, K. Shi, B. Yan, State damping control: A novel simple method of rotor UAV with high performance, IEEE access 8 (2020) 214346–214357, https://doi.org/10.1109/ACCESS.2020.3040779.
[26] Y. Du, N. Pan, Z. Xu, F. Deng, Y. Shen, H. Kang, Pavement distress detection and classification based on YOLO network, Int. J. Pavement Eng. (2020) 1–14, https://doi.org/10.1080/10298436.2020.1714047.
[27] Y. Yerdesh, Z. Abdulina, A. Aliuly, Y. Belyayev, M. Mohanraj, A. Kaltayev, Numerical simulation on solar collector and cascade heat pump combi water heating systems in Kazakhstan climates, Renew. Energy 145 (2020) 1222–1234.
[28] M.-W. Tian, S. Rostami, S. Aghakhani, A.S. Goldanlou, C. Qi, Investigation of 2D and 3D configurations of fins and their effects on heat sink efficiency of MHD hybrid nanofluid with slip and non-slip flow, Int. J. Mech. Sci. (2020), 105975.
[29] G. Cheraghian, S. Khalili Nezhad, S. Bazgir, Improvement of thermal stability of polyacryl amide solution used as a nano-fluid in enhanced oil recovery process by nanoclay, Int. J. Nanosci. Nanotechnol. 11 (2015) 201–208.
[30] G. Cheraghian, Improved Heavy Oil Recovery by Nanofluid Surfactant Flooding-An Experimental Study, European Association of Geoscientists & Engineers, 2016, pp. 1–5, 2016.
[31] M. Bahrami, M. Akbari, S.A. Bagherzadeh, A. Karimipour, M. Afrand, M. Goodarzi, Develop 24 dissimilar ANNs by suitable architectures & training algorithms via sensitivity analysis to better statistical presentation: measure MSEs between targets & ANN for Fe–CuO/Eg–Water nanofluid, Phys. Stat. Mech. Appl. 519 (2019) 159–168.
[32] A.H. Pordanjani, S. Aghakhani, Numerical investigation of natural convection and irreversibilities between two inclined concentric cylinders in presence of uniform magnetic field and radiation, Heat Tran. Eng. (2021) 1–21.
[33] M. Abareshi, E.K. Goharshadi, S.M. Zebarjad, H.K. Fadafan, A. Youssefi, Fabrication, characterization and measurement of thermal conductivity of Fe_3O_4 nanofluids, J. Magn. Magn Mater. 322 (2010) 3895–3901.
[34] S.O. Giwa, M. Sharifpur, M. Goodarzi, H. Alsulami, J.P. Meyer, Influence of base fluid, temperature, and concentration on the thermophysical properties of hybrid nanofluids of alumina–ferrofluid: experimental data, modeling through enhanced ANN, ANFIS, and curve fitting, J. Therm. Anal. Calorim. 143 (2021) 4149–4167.
[35] A.H. Pordanjani, A. Jahanbakhshi, A.A. Nadooshan, M. Afrand, Effect of two isothermal obstacles on the natural convection of nanofluid in the presence of magnetic field inside an enclosure with sinusoidal wall temperature distribution, Int. J. Heat Mass Tran. 121 (2018) 565–578.
[36] M. Hemmat Esfe, H. Rostamian, S. Esfandeh, M. Afrand, Modeling and prediction of rheological behavior of Al_2O_3-MWCNT/5W50 hybrid nano-lubricant by artificial neural network using experimental data, Phys. Stat. Mech. Appl. 510 (2018) 625–634.
[37] A. Hajatzadeh Pordanjani, S. Aghakhani, M. Afrand, B. Mahmoudi, O. Mahian, S. Wongwises, An updated review on application of nanofluids in heat exchangers for saving energy, Energy Convers. Manag. 198 (2019), 111886.
[38] I.D. Garbadeen, M. Sharifpur, J.M. Slabber, J.P. Meyer, Experimental study on natural convection of MWCNT-water nanofluids in a square enclosure, Int. Commun. Heat Mass Tran. 88 (2017) 1–8.
[39] M. Ibrahim, T. Saeed, Y.-M. Chu, H.M. Ali, G. Cheraghian, R. Kalbasi, Comprehensive study concerned graphene nano-sheets dispersed in ethylene glycol: experimental study and theoretical prediction of thermal conductivity, Powder Technol. 386 (2021) 51–59.
[40] J. Singh, R. Kumar, M. Gupta, H. Kumar, Thermal conductivity analysis of GO-CuO/DW hybrid nanofluid, Mater. Today: Proceedings 28 (3) (2020) 1714–1718.
[41] R. Ranjbarzadeh, A. Akhgar, S. Musivand, M. Afrand, Effects of graphene oxide-silicon oxide hybrid nanomaterials on rheological behavior of water at various time durations and temperatures: synthesis, preparation and stability, Powder Technol. 335 (2018) 375–387.
[42] M. Elkelawy, S.E.-d.H. Etaiw, M.I. Ayad, H. Marie, M. Dawood, H. Panchal, et al., An enhancement in the diesel engine performance, combustion, and emission attributes fueled by diesel-biodiesel and 3D silver thiocyanate nanoparticles additive fuel blends, J. Taiwan Instit. Chem. Eng. 124 (2021) 369–380.
[43] R. Walvekar, Y.Y. Chen, R. Saputra, M. Khalid, H. Panchal, D. Chandran, et al., Deep eutectic solvents-based CNT nanofluid – A potential alternative to conventional heat transfer fluids, J. Taiwan Instit. Chem. Eng. (1876–1070) (2021).
[44] S.-R. Yan, S. Aghakhani, A. Karimipour, Influence of a membrane on nanofluid heat transfer and irreversibilities inside a cavity with two constant-temperature semicircular sources on the lower wall: applicable to solar collectors, Phys. Scripta 95 (2020), 085702.
[45] Y. Zheng, S. Yaghoubi, A. Dezfulizadeh, S. Aghakhani, A. Karimipour, I. Tlili, Free convection/radiation and entropy generation analyses for nanofluid of inclined square enclosure with uniform magnetic field, J. Therm. Anal. Calorim. 141 (2020) 635–648.
[46] E. Shahsavani, M. Afrand, R. Kalbasi, Using experimental data to estimate the heat transfer and pressure drop of non-Newtonian nanofluid flow through a circular tube: Applicable for use in heat exchangers, Appl. Therm. Eng. 129 (2018) 1573–1581.
[47] M.S. Dehaj, M.Z. Mohiabadi, Experimental investigation of heat pipe solar collector using MgO nanofluids, Sol. Energy Mater. Sol. Cell. 191 (2019) 91–99.
[48] M.A. Sharafeldin, G. Gróf, Efficiency of evacuated tube solar collector using WO_3/Water nanofluid, Renew. Energy 134 (2019) 453–460.
[49] A. Wahab, A. Hassan, M.A. Qasim, H.M. Ali, H. Babar, M.U. Sajid, Solar energy systems – potential of nanofluids, J. Mol. Liq. 289 (2019), 111049.
[50] G. Cheraghian, Q. Wu, M. Mostofi, M.-C. Li, M. Afrand, J.S. Sangwai, Effect of a novel clay/silica nanocomposite on water-based drilling fluids: improvements in rheological and filtration properties, Colloid. Surface. Physicochem. Eng. Aspect. 555 (2018) 339–350.
[51] M.H. Esfe, S. Esfandeh, M. Afrand, M. Rejvani, S.H. Rostamian, Experimental evaluation, new correlation proposing and ANN modeling of thermal properties of EG based hybrid nanofluid containing ZnO-DWCNT nanoparticles for internal combustion engines applications, Appl. Therm. Eng. 133 (2018) 452–463.
[52] F. Zhou, J. Ji, W. Yuan, X. Zhao, S. Huang, Study on the PCM flat-plate solar collector system with antifreeze characteristics, Int. J. Heat Mass Tran. 129 (2019) 357–366.
[53] M.M. Abd El-Samie, X. Ju, C. Xu, X. Du, Q. Zhu, Numerical study of a photovoltaic/thermal hybrid system with nanofluid based spectral beam filters, Energy Convers. Manag. 174 (2018) 686–704.
[54] V. Bianco, F. Scarpa, L.A. Tagliafico, Numerical analysis of the Al_2O_3-water nanofluid forced laminar convection in an asymmetric heated channel for application in flat plate PV/T collector, Renew. Energy 116 (2018) 9–21.
[55] M. Asadi, A. Asadi, S. Aberoumand, An experimental and theoretical investigation on the effects of adding hybrid nanoparticles on heat transfer efficiency and pumping power of an oil-based nanofluid as a coolant fluid, Int. J. Refrig. 89 (2018) 83–92.
[56] M.-W. Tian, H. Moria, L.W.W. Mihardjo, A. Kaood, H. Sadighi Dizaji, K. Jermsittiparsert, Experimental thermal/economic/exergetic evaluation of hot/cold water production process by thermoelectricity, J. Clean. Prod. 271 (2020), 122923.
[57] M. Ghalandari, A. Maleki, A. Haghighi, M. Safdari Shadloo, M. Alhuyi Nazari, I. Tlili, Applications of nanofluids containing carbon nanotubes in solar energy systems: A review, J. Mol. Liq. 313 (2020), 113476.
[58] M. Bahiraei, S. Heshmatian, Thermal performance and second law characteristics of two new microchannel heat sinks operated with hybrid nanofluid containing graphene–silver nanoparticles, Energy Convers. Manag. 168 (2018) 357–370.
[59] M. Bahiraei, S. Heshmatian, M. Keshavarzi, A decision-making based method to optimize energy efficiency of ecofriendly nanofluid flow inside a new heat sink enhanced with flow distributor, Powder Technol. 342 (2019) 85–98.
[60] M. Hemmat Esfe, H. Rostamian, A. Shabani-samghabadi, A.A. Abbasian Arani, Application of three-level general factorial design approach for thermal conductivity of MgO/water nanofluids, Appl. Therm. Eng. 127 (2017) 1194–1199.
[61] H. Khodadadi, D. Toghraie, A. Karimipour, Effects of nanoparticles to present a statistical model for the viscosity of MgO-Water nanofluid, Powder Technol. 342 (2019) 166–180.

[62] K. Jafari, M.H. Fatemi, A.P. Toropova, A.A. Toropov, Correlation Intensity Index (CII) as a criterion of predictive potential: Applying to model thermal conductivity of metal oxide-based ethylene glycol nanofluids, Chem. Phys. Lett. 754 (2020), 137614.
[63] Y. Li, R. Kalbasi, Q. Nguyen, M. Afrand, Effects of sonication duration and nanoparticles concentration on thermal conductivity of silica-ethylene glycol nanofluid under different temperatures: An experimental study, Powder Technol. 367 (2020) 464–473.
[64] M.S. Hossain, A.K. Pandey, M.A. Tunio, J. Selvaraj, K.E. Hoque, N.A. Rahim, Thermal and economic analysis of low-cost modified flat-plate solar water heater with parallel two-side serpentine flow, J. Therm. Anal. Calorim. 123 (2016) 793–806.
[65] A. Ibrahim, A. Fudholi, K. Sopian, M.Y. Othman, M.H. Ruslan, Efficiencies and improvement potential of building integrated photovoltaic thermal (BIPVT) system, Energy Convers. Manag. 77 (2014) 527–534.
[66] S.R. Park, A.K. Pandey, V.V. Tyagi, S.K. Tyagi, Energy and exergy analysis of typical renewable energy systems, Renew. Sustain. Energy Rev. 30 (2014) 105–123.
[67] K. Sudhakar, Tulika Srivastava, Energy and Exergy Analysis of 36 W Solar Photovoltaic Module, vol. 35, Taylor & Francis, 2014, pp. 51–57.
[68] A. Nahar, M. Hasanuzzaman, N.A. Rahim, Numerical and experimental investigation on the performance of a photovoltaic thermal collector with parallel plate flow channel under different operating conditions in Malaysia, Sol. Energy 144 (2017) 517–528.
[69] M.M. Rahman, M. Hasanuzzaman, N.A. Rahim, Effects of operational conditions on the energy efficiency of photovoltaic modules operating in Malaysia, J. Clean. Prod. 143 (2017) 912–924.
[70] M. Hazami, A. Riahi, F. Mehdaoui, O. Nouicer, A. Farhat, Energetic and exergetic performances analysis of a PV/T (photovoltaic thermal) solar system tested and simulated under to Tunisian (North Africa) climatic conditions, Energy 107 (2016) 78–94.
[71] S. Kumar, G.N. Tiwari, Life cycle cost analysis of single slope hybrid (PV/T) active solar still, Appl. Energy 86 (2009) 1995–2004.
[72] B. Leland, T. Anthony, Engineering Economy, fourth ed., Book, 1998, pp. 46–161, 0-070-115964-9.
[73] M.R. Saffarian, M. Moravej, M.H. Doranehgard, Heat transfer enhancement in a flat plate solar collector with different flow path shapes using nanofluid, Renew. Energy 146 (2020) 2316–2329.
[74] https://www.meteoblue.com/en/weather/historyclimate/climatemodelled/china_united-states-of-america_4960817.
[75] F. Esmaeilzadeh, A.S. Teja, A. Bakhtyari, The thermal conductivity, viscosity, and cloud points of bentonite nanofluids with n-pentadecane as the base fluid, J. Mol. Liq. 300 (2020), 112307.
[76] https://www.us-nano.com/inc/sdetail/623, 2021.